Supporting Information

Mitigating Magnetic Frustration to Improve Single-Crystalline Nonstoichiometric $Li_{1.06}Ni_{0.90}Mn_{0.04}O_2$ for Lithium-Ion Batteries

Guoyu Ding[a†], Shizhou Wang[a†], Xinhui Huang[a], Qiancheng Zhao[a], Yiyang Peng[a], Zhonghan Wu[a], Na Jiang[a], Kuiming Liu[a], Yudong Zhang[a], Zhichen Hou[a], Wutong Yang[a], Meng Yu[a,b], Fangming Liu[a,], Fangyi Cheng[a,b,c,*]*

a. Key Laboratory of Advanced Energy Materials Chemistry (Ministry of Education), Engineering Research Center of High-efficiency Energy Storage (Ministry of Education), College of Chemistry, Nankai University, Tianjin 300071, China.

b. State Key Laboratory of Advanced Chemical Power Sources, Nankai University, Tianjin 300071, China.

c. Haihe Laboratory of Sustainable Chemical Transformations, Tianjin 300192, China.

† These authors contributed equally to this work.

** Corresponding authors.*

E-mail: fmliu@nankai.edu.cn (F.L.); fycheng@nankai.edu.cn (F.C.)

Supplemental Figures

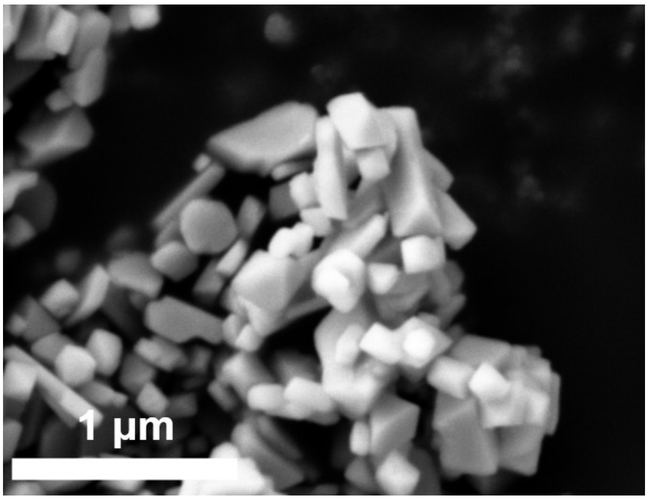

Fig. S1. SEM image of LP-NM particles.

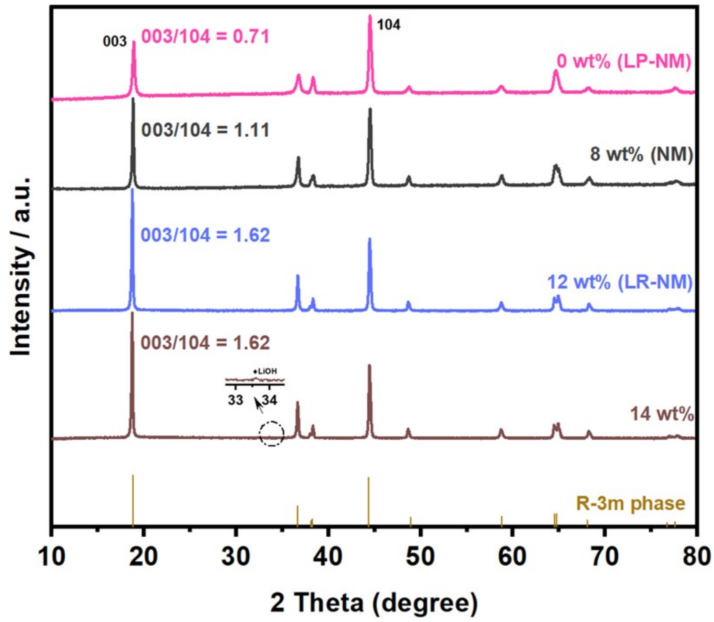

Fig. S2. The XRD patterns for the samples at different lithium supplement.

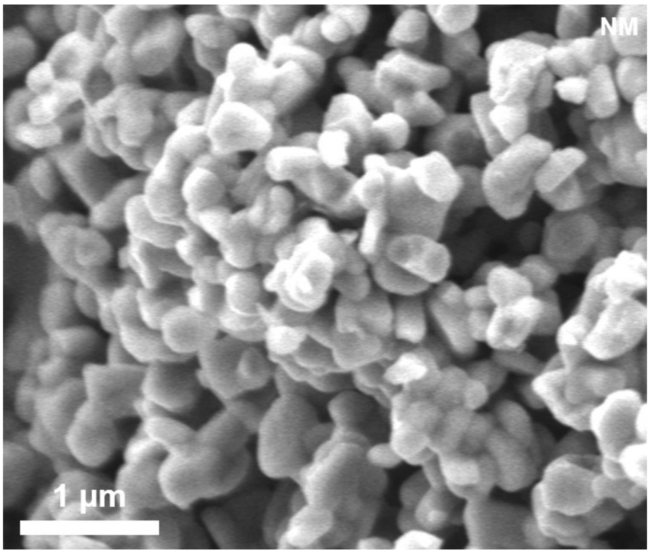

Fig. S3. SEM image of NM particles.

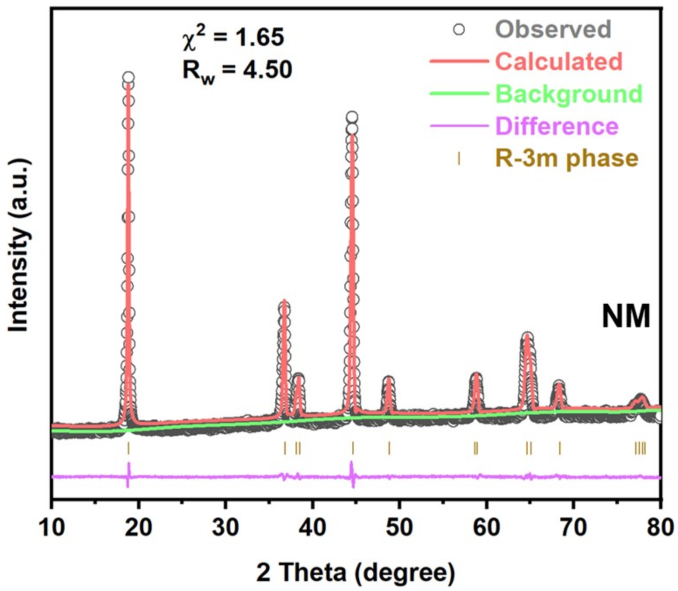

Fig. S4. Rietveld-refined XRD patterns of NM.

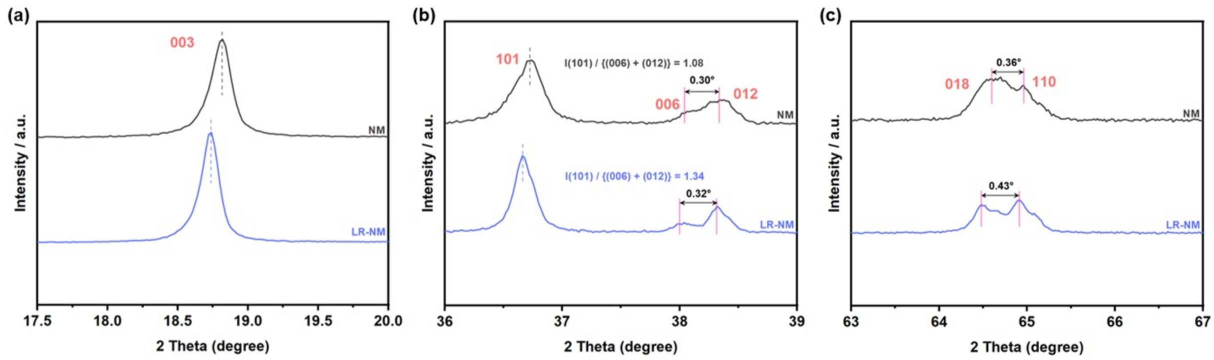

Fig. S5. XRD patterns of expanded view region of 2θ at (a) 17.5°–20.0°, (b) 36.0°–39.0°, and (c) 63.0°–67.0°.

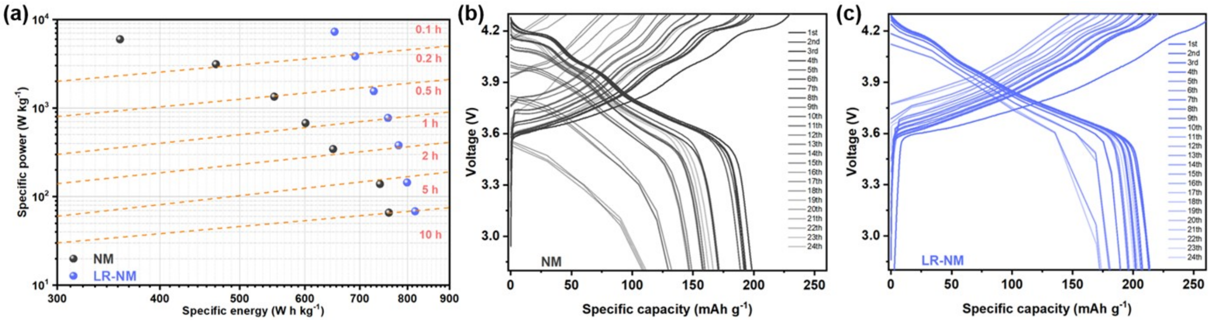

Fig. S6. Ragone diagram of NM and LR-NM (a). The charge discharge curves for the rate performance of NM (b) and LR-NM (c).

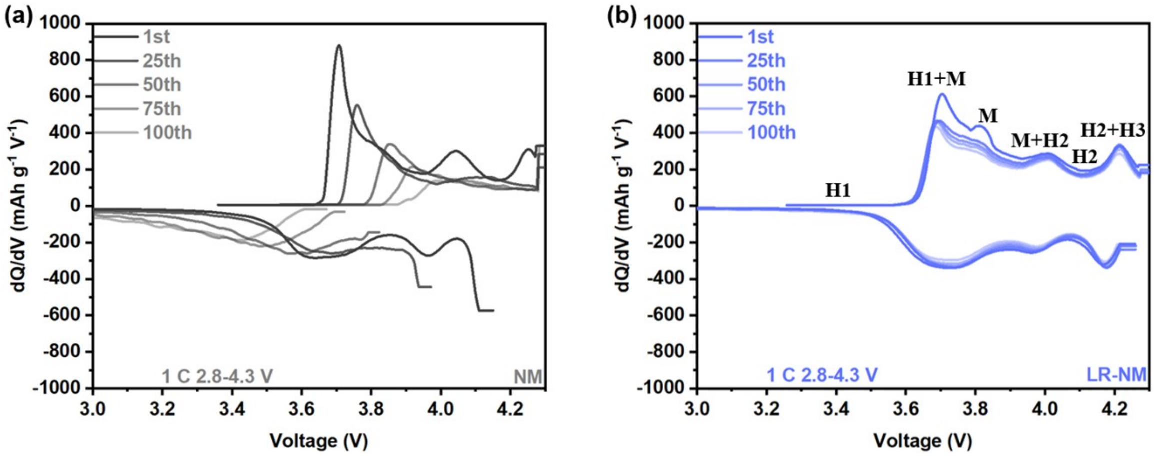

Fig. S7. dQ dV^{-1} curves for (a) NM and (b) LR-NM at different cycles.

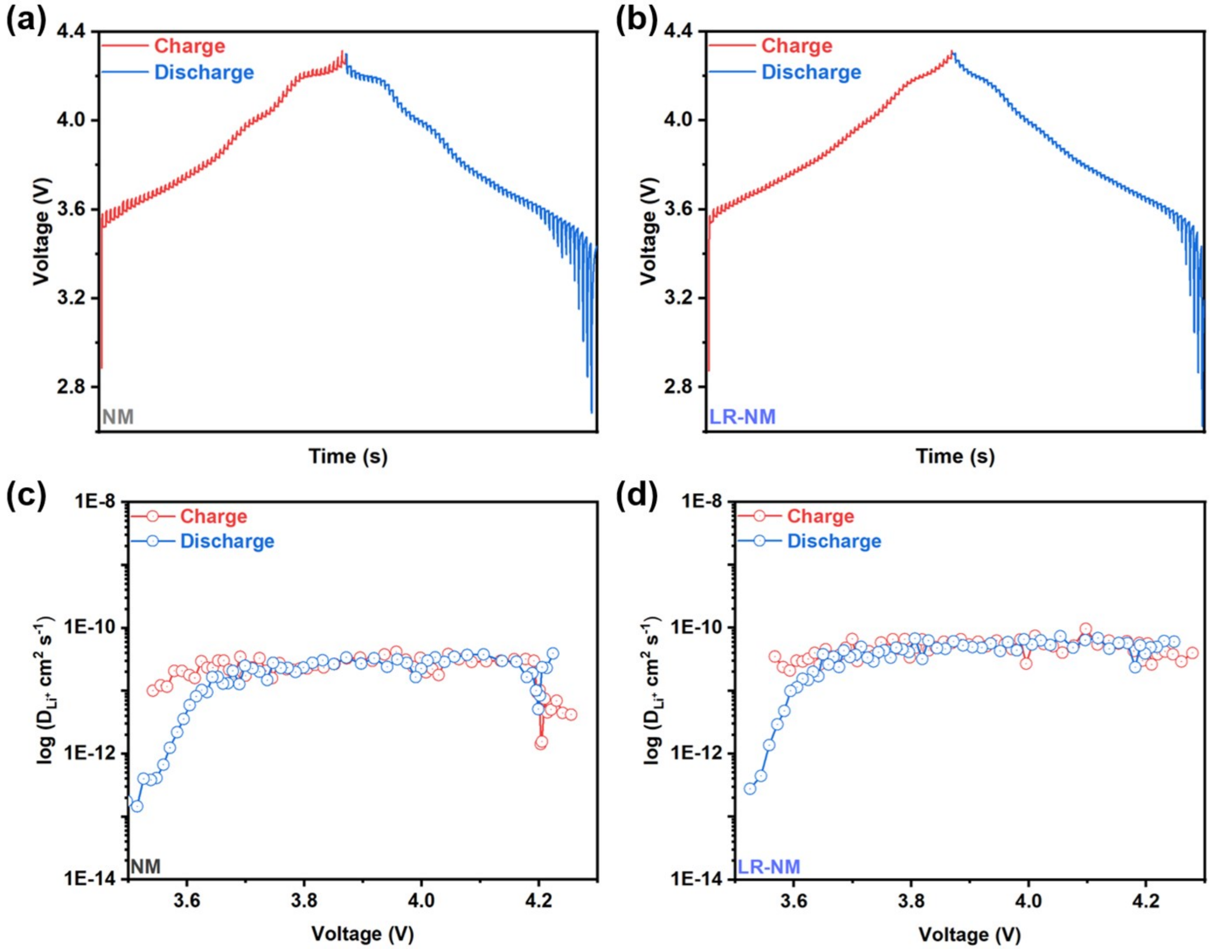

Fig. S8. GITT curves (a, b) and the calculated Li^+ diffusion coefficient (c, d) of NM and LR-NM.

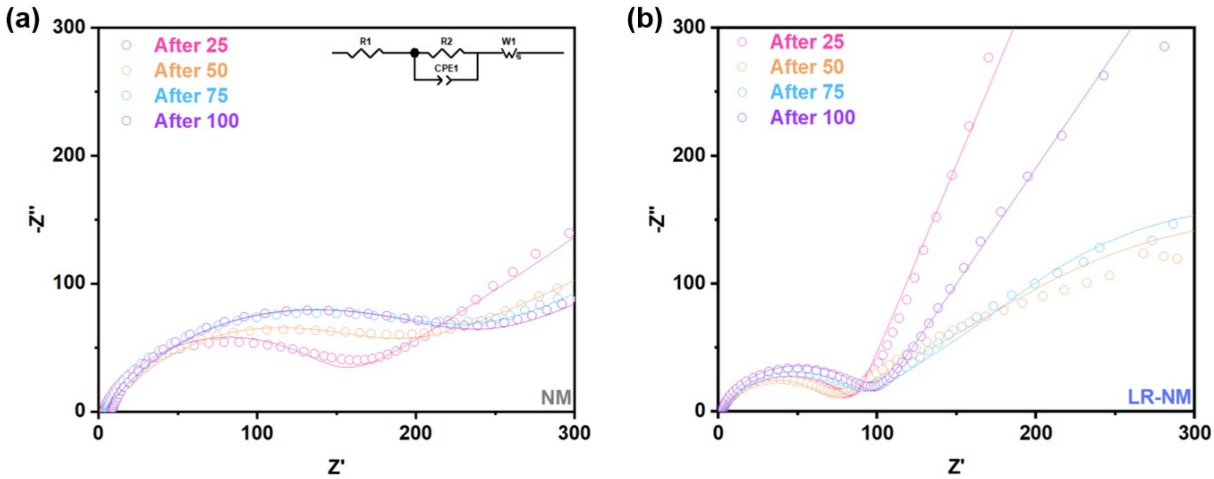

Fig. S9. Nyquist plots of different numbers of cycles at 1 C for (a) NM and (b) LR-NM in the voltage range of 2.8–4.3 V.

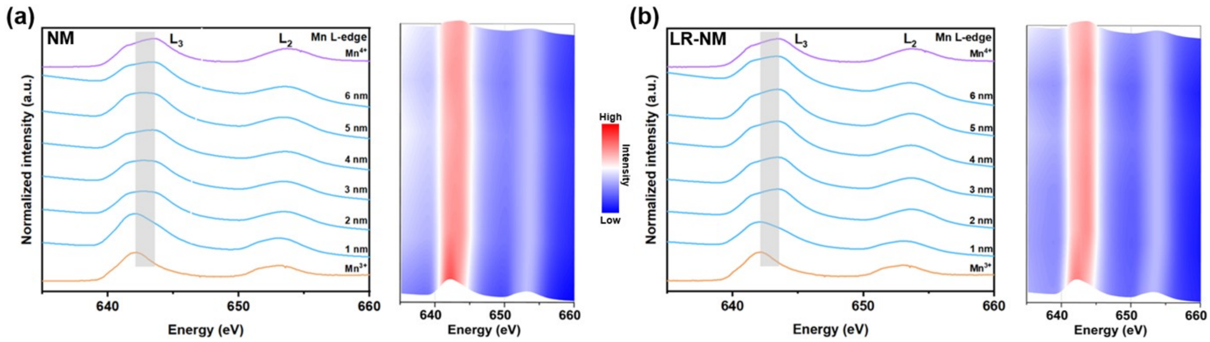

Fig. S10. Mn L-edge EELS spectra of the pristine NM (a) and LR-NM (b).

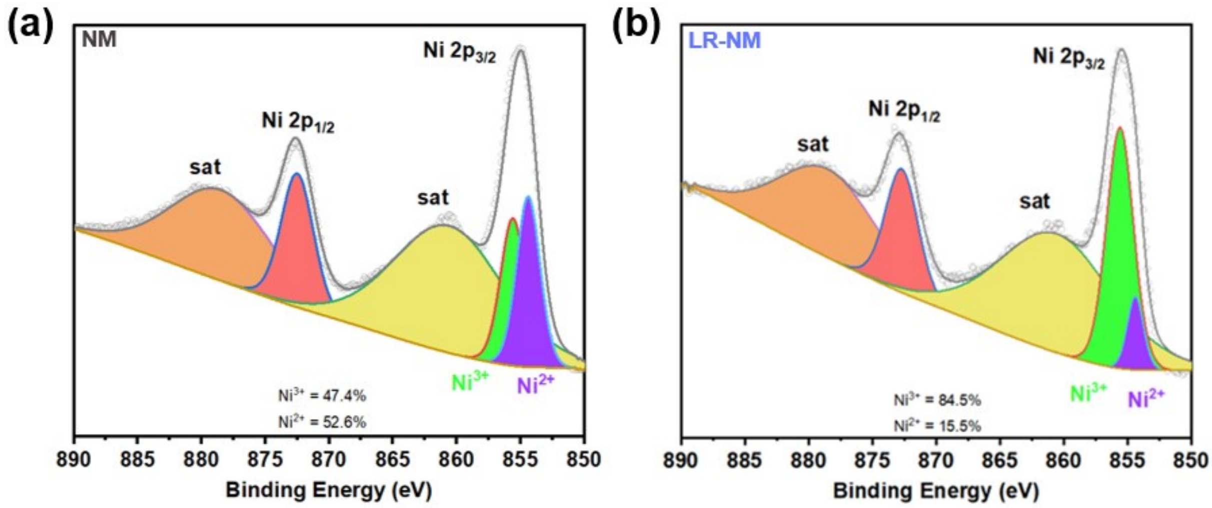

Fig. S11. XPS spectra of Ni 2p for NM (a) and LR-NM (b) cathodes.

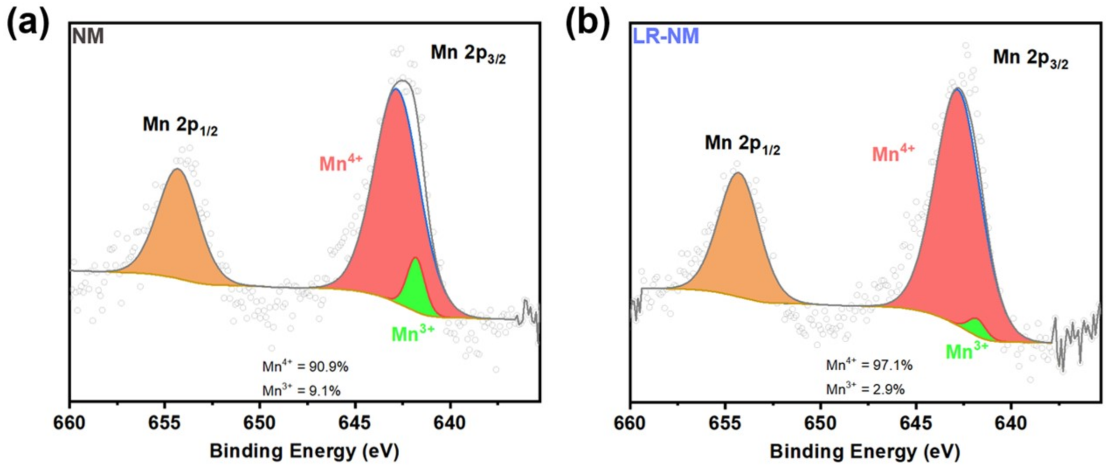

Fig. S12. XPS spectra of Mn 2p for NM (a) and LR-NM (b) cathodes.

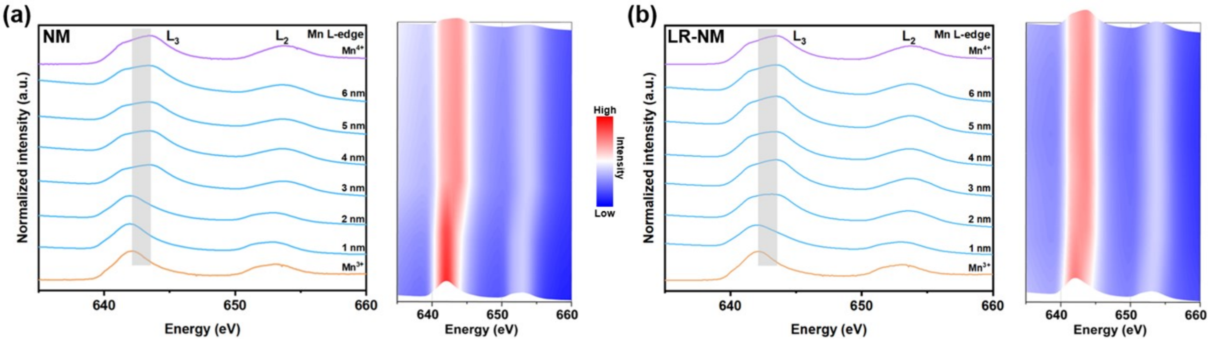

Fig. S13. Mn L-edge EELS spectra of the NM (a) and LR-NM (b) after 100 cycles.

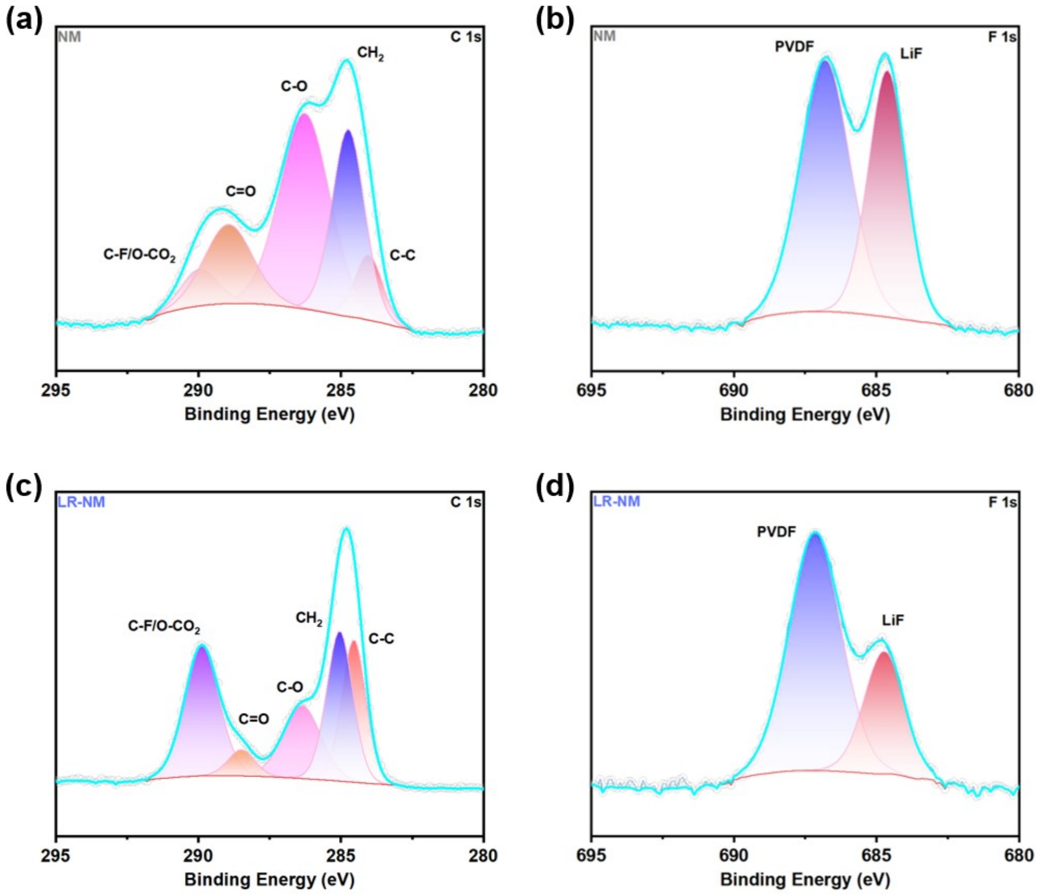

Fig. S14. C 1s, and F 1s XPS spectra for NM (a and b) and LR-NM (c and d) at 1 C rate after 100 cycles.

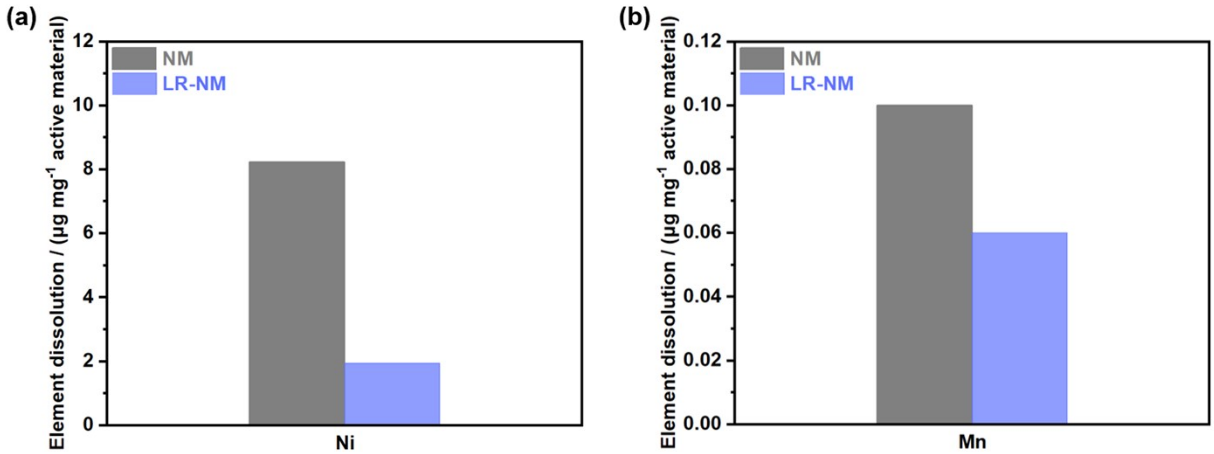

Fig. S15. Dissolution of (a) Ni and (b) Mn elements for NM and LR-NM from anode after 100 cycles.

Table S1. Elemental analysis of the samples using ICP-OES.

Sample	Li (molar ratio)	Ni (molar ratio)	Mn (molar ratio)
$Ni_{0.95}Mn_{0.05}(OH)_x$ precursor	/	0.95	0.05
NM	0.99	0.96	0.05
LR-NM	1.06	0.90	0.04

Table S2. Rietveld refinement data of XRD for NM and LR-NM.

Sample	Lattice parameters			Ni in Li site (%)	Rw (%)	χ^2 (%)
	a (Å)	c (Å)	c/a			
NM	2.867	14.165	4.9407	6.86	4.50	1.65
LR-NM	2.869	14.177	4.9414	1.51	3.25	1.37

Table S3. The performance comparison and mechanistic discussion of reported nickel-rich oxide cathode materials.

Composition	Initial discharge capacity (mAh g^{-1})	Voltage range (V)	Cycle number	Capacity retention (%)	Ref.
SC-$Li_{1.06}Ni_{0.90}Mn_{0.04}O_2$	214.8 (0.1 C)	2.8-4.3	100	89.5 (1 C)	This
			100	93.4 (5 C)	work
SC-$LiNi_{0.95}Mn_{0.05}O_2$	218.2 (0.1 C)	2.7-4.3	200	84.4 (1 C)	1
			400	54.5 (5 C)	
PC-$LiNi_{0.95}Mn_{0.05}O_2$	217.2 (0.1 C)	2.75-4.3	100	89.9 (1 C)	2
Co coated/doped	221.2 (0.1 C)	3.0-4.3	100	83.2 (0.5 C)	3
PC-$LiNi_{0.95}Mn_{0.05}O_2$					
PPy coated	234.6 (0.05 C)	2.7-4.3	100	90.1	4
PC-$LiNi_{0.95}Mn_{0.05}O_2$			100	91.1	
Al doped	/	2.7-4.3 V	180	89.4 (1 C)	5
PC-$LiNi_{0.90}Mn_{0.10}O_2$			100	86.4 (5 C)	
Co, Al co-doped	/	3.0-4.3	200	80.4 (1 C)	6
PC-$LiNi_{0.90}Mn_{0.10}O_2$			200	76.8 (5 C)	
Co doped and La_2O_3	214.7 (0.2 C)	2.7-4.3	200	77.9 (1 C)	7
coated			200	75.7 (5 C)	
PC-$LiNi_{0.90}Mn_{0.10}O_2$					
La doped and La_2O_3	214.4 (0.2 C)	2.7-4.3	100	83.19 (1 C)	8
coated					
PC-$LiNi_{0.90}Mn_{0.10}O_2$					

Table S4. The average charging/discharging Li^+ diffusion coefficient of NM and LR-NM electrodes.

Sample	NM	LR-NM
Charging / $cm^2\ s^{-1}$	2.21×10^{-11}	4.74×10^{-11}
Discharging / $cm^2\ s^{-1}$	1.91×10^{-11}	4.08×10^{-11}

Table S5. Impedance parameters fitted at various cycles for NM and LR-NM electrodes.

Sample	25th cycle		50th cycle		75th cycle		100th cycle	
	R_{sf} (Ω)	R_{ct} (Ω)	R_{sf} (Ω)	R_{ct} (Ω)	R_{sf} (Ω)	R_{ct} (Ω)	R_{sf} (Ω)	R_{ct} (Ω)
NM	3.5	130.2	3.0	135.1	2.1	182.9	3.1	193.7
LR-NM	2.4	82.7	1.8	60.5	2.1	80.4	1.6	93.9

Notes and references

1. L. Ni, R. Guo, S. Fang, J. Chen, J. Gao, Y. Mei, S. Zhang, W. Deng, G. Zou, H. Hou and X. Ji, *eScience*, 2022, **2**, 116-124.
2. Y. Wang, Y. Zhu and P. Gao, *Electrochim. Acta*, 2022, **427**, 140891.
3. J. Chen, B. Chu, G. Li, T. Huang and A. Yu, *Electrochem Commun*, 2023, **152**, 107514.
4. P. He, M. Zhang, S. Wang, L. Yuwen, Y. Wang, Y. Yan, D. Zhang and X. Sun, *Electrochim. Acta*, 2023, **470**, 143331.
5. H. Feng, Y. Leng, T. Chen, Y. Sun, C. Hai and Y. Zhou, *J. Alloy. Compd.*, 2023, **960**, 170676.
6. Z. Xiao, B. Zhang, X. He and X. Ou, *Chem. Commun.*, 2023, **59**, 7935-7938.
7. J.-Q. Peng, Y.-Y. Wei, D.-M. Liu, Y. Li, B. Hu, B. Huang, J.-W. Yang, S.-H. Xiao and R.-H. Wang, *Rare Met.*, 2023, **43**, 658-670.
8. J. Peng, Y. Wei, B. Hu, L. Zhang, J. Huang, H. Tang, B. Huang, Y. Li, S. Chen and S. Xiao, *Ionics*, 2023, **29**, 2549-2561.